NASA Technical Memorandum 102874

An Eigenvalue Analysis of Finite-Difference Approximations for Hyperbolic IBVPs II: The Auxiliary Dirichlet Problem

Robert F. Warming and Richard M. Beam

November 1990

NASA
National Aeronautics and Space Administration

NASA Technical Memorandum 102874

An Eigenvalue Analysis of Finite-Difference Approximations for Hyperbolic IBVPs II: The Auxiliary Dirichlet Problem

Robert F. Warming and Richard M. Beam
Ames Research Center, Moffett Field, California

November 1990

National Aeronautics and
Space Administration

Ames Research Center
Moffett Field, California 94035-1000

AN EIGENVALUE ANALYSIS OF FINITE-DIFFERENCE APPROXIMATIONS FOR HYPERBOLIC IBVPs II: THE AUXILIARY DIRICHLET PROBLEM[1]

ROBERT F. WARMING AND RICHARD M. BEAM

NASA AMES RESEARCH CENTER, MOFFETT FIELD, CA 94035, USA

ABSTRACT

The matrix eigenvalue problem for a discrete hyperbolic initial-boundary-value problem reduces to the eigenvalue analysis of a banded quasi-Toeplitz matrix. A direct analysis is, in general, analytically intractable and numerically unreliable. An asymptotic (large matrix order) approach partitions the eigenvalue analysis into two parts, namely the analysis for the boundary condition *independent* eigenvalues and the analysis for the boundary condition *dependent* eigenvalues. The boundary condition independent spectrum is associated with an auxiliary Dirichlet problem, i.e., the spectrum of a banded Toeplitz matrix. The boundary condition dependent spectrum is associated with the normal modes of the Godunov-Ryabenkii and the Gustafsson-Kreiss-Sundström stability theory; however, eigenvalues not considered in the stability theory (i.e., *stable* eigenvalues) may be part of the boundary condition dependent spectrum. In this paper we describe a method for determining the eigenvalue spectra for banded Toeplitz and quasi-Toeplitz matrices of large order. The algorithm for the asymptotic spectrum also leads to a simple similarity transformation that allows reliable numerical eigenvalue computations for banded Toeplitz and quasi-Toeplitz matrices of any order.

1. INTRODUCTION

Finite-difference approximations of hyperbolic *initial-boundary-value problems* (IBVPs) require *numerical boundary schemes* (NBSs) in addition to the analytical boundary conditions specified for the differential equation. An interior difference approximation together with the required analytical boundary conditions and NBSs is referred to as a *discrete* IBVP. The eigenvalue spectrum associated with a discrete IBVP plays a crucial role in the stability analysis and in the actual computational performance of the approximation. For example, the asymptotic temporal behavior of the solution on a fixed spatial grid is dependent on the eigenvalue spectrum. However, for a discrete IBVP on a finite domain, the eigenvalue or normal mode analysis is, in general, analytically intractable. Furthermore, standard numerical eigenvalue routines often fail to give reliable results as the mesh is refined, i.e., as the order of the matrix (associated with the discrete IBVP) increases.

A classical method for carrying out a stability analysis of a discrete hyperbolic IBVP is the normal mode analysis of Godunov and Ryabenkii (GR) [2] and Gustafsson, Kreiss, and Sundström (GKS) [4]. The stability theory avoids the analytical intractability of the normal mode analysis for the finite-domain IBVP by using an asymptotic approach which leads to the analysis of the Cauchy problem and related quarter-plane problems.

[1]Preprint for the Third International Conference on Hyperbolic Problems, Uppsala, Sweden, June 11-15, 1990

Determination of the finite-domain eigenvalue spectrum is not part of the GR and GKS stability theory.

In this paper we follow the approach of the stability theory and find the asymptotic (large matrix order) eigenvalue spectrum for the IBVP. The asymptotic approach partitions the eigenvalue analysis into two parts, namely the analysis for the boundary condition *independent* eigenvalues and the analysis for the boundary condition *dependent* eigenvalues. The boundary condition independent spectrum is associated with an auxiliary Dirichlet problem, i.e., the spectrum of a banded Toeplitz matrix. (A matrix whose entries are constant along each diagonal is called a *Toeplitz* matrix). The boundary condition dependent spectrum is associated with the quarter-plane modes of the GR and GKS stability theory; however, eigenvalues not considered in the stability theory (i.e., *stable* eigenvalues) may be part of the eigenvalue spectrum. With the exception of isolated eigenvalues detected by the boundary condition dependent analysis, the asymptotic eigenvalue spectrum of a discrete IBVP is the eigenvalue spectrum of a banded Toeplitz matrix corresponding to the auxiliary Dirichlet problem.

For a tridiagonal Toeplitz matrix, the eigenvalues are known analytically [8,1]. (In [10] we considered the Lax-Wendroff scheme as a prototypical method where the bandwidth of the corresponding Toeplitz matrix is three.) If the bandwidth of a Toeplitz matrix is larger than three, the eigenvalues cannot be determined analytically. Although the finite-domain eigenvalue problem is reduced to the study of auxiliary eigenvalue problems, we are still faced with an intractable analytical problem. In this paper we describe an algorithm for determining the asymptotic eigenvalue spectra for Toeplitz and quasi-Toeplitz matrices of arbitrary bandwidth. (A *quasi*-Toeplitz matrix is defined in Section 8.)

For simplicity, the description of the asymptotic analysis is presented in the context of the semi-discrete approximation for a model hyperbolic IBVP. The model hyperbolic equation is introduced in Section 2. In Section 3 a system of ordinary differential equations associated with a semi-discrete approximation is formulated for a prototypical spatial difference approximation. The normal mode analysis for the semi-discrete approximation of Section 3 is outlined in Section 4 to illustrate the analytical intractability of the finite-domain eigenvalue problem.

Next we consider the asymptotic (large matrix order) eigenvalue problem. The essential notion in the asymptotic analysis is to partition the eigenvalue spectrum into two groups. These two groups are related to auxiliary eigenvalue problems. Before outlining the asymptotic analysis, we define relevant auxiliary problems in Sections 5 through 8. The eigenvalue problem for banded Toeplitz and quasi-Toeplitz matrices is formulated in Section 9. The asymptotic eigenvalue spectrum for a quasi-Toeplitz matrix is partitioned into two groups in Section 10. An algorithm for the asymptotic eigenvalue spectrum is given in Section 11. In Section 12 we consider the cause of unreliable eigenvalues when standard numerical routines are applied to banded Toeplitz matrices. We trace the origin of the problem to exponentially growing eigenvectors. After a simple similarity transformation is applied to the matrix, we demonstrate that standard routines give accurate numerical results. Finally, additional spectral plots are examined in Section 13.

2. IBVP FOR A MODEL HYPERBOLIC EQUATION

For simplicity we consider the scalar hyperbolic equation

$$\frac{\partial u}{\partial t} = c\frac{\partial u}{\partial x}, \quad 0 \le x \le L, \quad t > 0 \tag{2.1}$$

where $u = u(x,t)$ and $c > 0$ is a real constant. For a well-posed IBVP on a finite domain one must specify initial data, $u(x,0) = f(x)$, $0 \le x \le L$, and an *analytical* boundary condition at $x = L$,

$$u(L,t) = g(t) \quad \text{for} \quad c > 0. \tag{2.2}$$

3. A PROTOTYPICAL SEMI-DISCRETE APPROXIMATION

A semi-discrete approximation of (2.1) is obtained by dividing the spatial interval L into J subintervals of length Δx where $J\Delta x = L$, $x = x_j = j\Delta x$ and approximating the spatial derivative u_x by a difference quotient. As a prototypical approximation, we replace u_x by an uncentered third-order-accurate approximation:

$$\frac{du_j}{dt} = \frac{c}{\Delta x}(a_{-1}u_{j-1} + a_0 u_j + a_1 u_{j+1} + a_2 u_{j+2}) \tag{3.1a}$$

where

$$a_{-1} = -1/3, \quad a_0 = -1/2, \quad a_1 = 1, \quad a_2 = -1/6. \tag{3.1b}$$

The approximation (3.1) is called *semi*-discrete since the time variable is left continuous. On the right boundary ($x = L$) the solution is given by the analytical boundary condition (2.2). We assume that the boundary condition is homogeneous, i.e., $g(t) = 0$, and for the semi-discrete problem we write

$$u_J = 0. \tag{3.2}$$

If we apply the interior approximation (3.1) at the left (outflow) boundary ($j = 0$), then the stencil protrudes one point to the left of the boundary. It is clear that an additional numerical boundary scheme (NBS) is required. Gustafsson [3] has shown that there is no loss of accuracy if the order of an NBS is one order lower than the order of the interior approximation. Consequently at the left boundary we approximate u_x by a second-order-accurate *upwind* approximation:

$$\frac{du_0}{dt} = \frac{c}{\Delta x}(b_0 u_0 + b_1 u_1 + b_2 u_2), \quad \text{where} \quad b_0 = -3/2, \quad b_1 = 2, \quad b_2 = -1/2. \tag{3.3a,b}$$

For the purposes of analysis, it is convenient to rewrite the NBS (3.3) as an equivalent space extrapolation NBS:

$$q(E)u_{-1} = (E-1)^3 u_{-1} = 0 \tag{3.4}$$

where the shift operator E is defined by $Eu_j = u_{j+1}$ and $q(E)$ is a polynomial in E.

If the interior approximation (3.1) is applied at $j = J-1$, the computational stencil protrudes one point to the right of the *inflow* boundary ($j = J$). At the point $j = J-1$ we replace the approximation of u_x by a second-order-accurate centered approximation:

$$\frac{du_{J-1}}{dt} = \frac{c}{\Delta x}(c_{-1}u_{J-2} + c_0 u_{J-1} + c_1 u_J), \quad \text{where} \quad c_{-1} = -1/2, \; c_0 = 0, \; c_1 = 1/2. \tag{3.5a,b}$$

The NBS (3.5) is equivalent to the space extrapolation NBS

$$w(E)u_{J+1} = (1 - E^{-1})^3 u_{J+1} = 0. \tag{3.6}$$

The semi-discrete approximation (3.1) for $j = 1, 2, \cdots, J-2$ together with the boundary conditions (3.2), (3.3), and (3.5) can be written as a system of ordinary differential equations (ODEs) in vector-matrix form as

$$\frac{d\mathbf{u}}{dt} = \mathcal{A}\mathbf{u}, \quad \text{where} \quad \mathcal{A} = \frac{c}{\Delta x}\mathbf{A} \tag{3.7a,b}$$

and

$$\mathbf{u} = \begin{bmatrix} u_0 \\ u_1 \\ u_2 \\ \cdot \\ \cdot \\ \cdot \\ u_{J-3} \\ u_{J-2} \\ u_{J-1} \end{bmatrix}, \quad \mathbf{A} = \begin{bmatrix} b_0 & b_1 & b_2 & & & & & & \\ a_{-1} & a_0 & a_1 & a_2 & & & & & \\ & a_{-1} & a_0 & a_1 & a_2 & & O & & \\ & & \cdot & \cdot & \cdot & \cdot & & & \\ & & & \cdot & \cdot & \cdot & \cdot & & \\ & & & & \cdot & \cdot & \cdot & \cdot & \\ & & O & & & a_{-1} & a_0 & a_1 & a_2 \\ & & & & & & a_{-1} & a_0 & a_1 \\ & & & & & & & c_{-1} & c_0 \end{bmatrix}. \tag{3.8a,b}$$

The entry changes in the first and last rows are due to the NBSs (3.3) and (3.5). Here $\mathbf{A}$ is a $J \times J$ matrix.

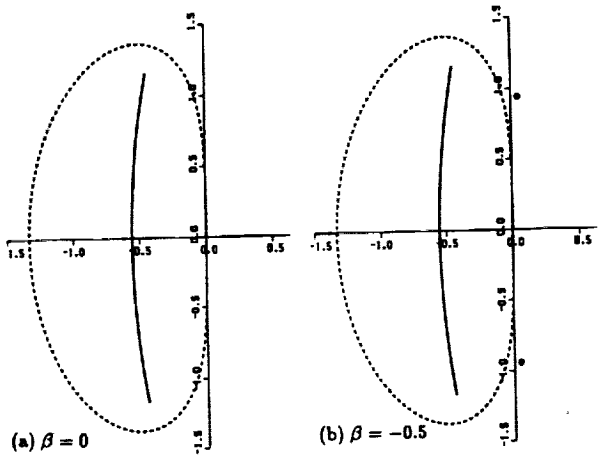

Fig. 3.1. Asymptotic eigenvalue spectra in the complex plane.

The asymptotic ($J \to \infty$) eigenvalue locus in the complex plane for the matrix (3.8b) is the *solid* curve in Fig. 3.1a. The eigenvalue locus is defined to be a curve (in the complex plane) through the eigenvalues. Since the locus shown in the figure is the asymptotic locus and the eigenvalue spectrum becomes dense on the locus as $J \to \infty$, we shall henceforth use the word spectrum rather than locus. The spectrum for the semi-discrete IBVP shown in Fig. 3.1a was computed numerically by a computational algorithm described in Section 11. The *dashed* oval curve is the eigenvalue spectrum for the Cauchy problem (Section 7).

The NBSs (3.3) and (3.5) do not introduce any boundary condition dependent modes. A simple way of introducing boundary condition dependent modes for the purpose of illustration is to generalize NBS (3.5) to

$$\frac{du_{J-1}}{dt} = \frac{c}{\Delta x}(c_{-2}u_{J-3} + c_{-1}u_{J-2} + c_0 u_{J-1} + c_1 u_J) \tag{3.9a}$$

where

$$c_{-2} = -\beta, \quad c_{-1} = 3\beta - 1/2, \quad c_0 = -3\beta, \quad c_1 = \beta + 1/2. \tag{3.9b}$$

If $\beta = 0$, then (3.9) reduces to (3.5). The semi-discrete IBVP formulated in this section with (3.9) as an NBS is GKS unstable if $\beta \leq -0.48$ [1]. For any value of β the asymptotic spectrum is the same as shown in Fig. 3.1a except for the possible addition of boundary condition dependent eigenvalues. As an example, for $\beta = -1/2$ there are two boundary condition dependent eigenvalues in the right half of the complex plane shown by the filled circles in Fig. 3.1b.

It should be emphasized that the eigenvalue analysis of this paper is independent of the origin of the matrix, e.g., the analysis is essentially the same for both the semi- and fully- discrete approximations.

4. NORMAL MODE ANALYSIS

The normal mode analysis leads directly to the eigenvalue problem. If we look for a solution of (3.7a) of the form

$$\mathbf{u}(t) = e^{\sigma t}\boldsymbol{\phi} \tag{4.1}$$

then we obtain

$$\mathcal{A}\boldsymbol{\phi} = \sigma\boldsymbol{\phi}. \tag{4.2}$$

But this is just the eigenvalue problem for the matrix $\mathcal{A}$ where $\boldsymbol{\phi}$ is the eigenvector and σ is the eigenvalue. In the eigenvalue analysis it is convenient to remove the $c/\Delta x$ dependence of the matrix $\mathcal{A}$. We use (3.7b) to rewrite (4.2) as

$$\mathbf{A}\boldsymbol{\phi} = \lambda\boldsymbol{\phi} \tag{4.3}$$

where $\lambda = \sigma\Delta x/c$.

For the eigenvalue analysis, we use the component form for the system of ordinary differential equations with space extrapolation NBSs. The system of equations is (3.1) for $j = 0, 1 \cdots, J-1$ and the boundary conditions are given by (3.4), (3.2), and (3.6):

$$q(E)u_{-1} = 0, \qquad u_J = 0, \qquad w(E)u_{J+1} = 0. \tag{4.4a,b,c}$$

We look for a solution of the form

$$u_j(t) = e^{\sigma t}\phi_j. \tag{4.5}$$

(Note that this equation is just the component form of (4.1).) Substitution of (4.5) into the interior approximation (3.1) and the boundary conditions (4.4) yields

$$\lambda\phi_j = a_{-1}\phi_{j-1} + a_0\phi_j + a_1\phi_{j+1} + a_2\phi_{j+2}, \quad j = 0, 1, \cdots, J-1 \tag{4.6}$$

and

$$q(E)\phi_{-1} = 0, \qquad \phi_J = 0, \qquad w(E)\phi_{J+1} = 0. \tag{4.7a,b,c}$$

Note that (4.6) is the generic equation of the system (4.3) excluding the first and last equation. Furthermore, one can easily show that (4.6) for $j = 0$ with ϕ_{-1} given by (4.7a) is equivalent to the first row of (4.3) where $\mathbf{A}$ is (3.8a).

Since (4.6) is a linear homogeneous difference equation for ϕ_j, one looks for a solution of the form

$$\phi_j = \kappa^j, \tag{4.8}$$

where κ is a complex constant, to obtain

$$\lambda = a_{-1}\kappa^{-1} + a_0 + a_1\kappa + a_2\kappa^2. \tag{4.9}$$

This is a cubic equation in κ and we denote the roots by κ_1, κ_2, and κ_3. Since (4.6) is a third-order difference equation, the general solution is (assuming distinct κ's)

$$\phi_j = \alpha_1\kappa_1^j + \alpha_2\kappa_2^j + \alpha_3\kappa_3^j. \tag{4.10}$$

The constants (α_ℓ's) are determined by substituting (4.10) in the boundary conditions (4.7). One obtains a characteristic equation of order J relating κ_1, κ_2, and κ_3. In general, one cannot solve for the roots of the characteristic equation which accounts for the analytic intractability of the normal mode analysis on a finite domain.

Before continuing with the asymptotic analysis, we define relevant auxiliary problems in the next four sections.

5. AN AUXILIARY DIRICHLET PROBLEM

The auxiliary Dirichlet problem is constructed by replacing all requisite boundary conditions by *over-specified* homogeneous Dirichlet boundary conditions. In other words, any grid function value u_j required by the interior difference approximation which falls outside the computational domain $0 \le x \le L$ is replaced by zero.

As an example we consider the semi-discrete approximation of Section 3. The auxiliary Dirichlet problem is obtained by setting the polynomial operators $q(E)$ and $w(E)$ in (4.4) to unity, i.e., the boundary conditions for the auxiliary Dirichlet problem are

$$u_{-1} = 0, \qquad u_J = 0, \qquad u_{J+1} = 0. \tag{5.1a,b,c}$$

The matrix corresponding to the auxiliary Dirichlet problem is

$$\mathbf{A} = \begin{bmatrix} a_0 & a_1 & a_2 & & & & & & \\ a_{-1} & a_0 & a_1 & a_2 & & & & & \\ & a_{-1} & a_0 & a_1 & a_2 & & O & & \\ & & \cdot & \cdot & \cdot & \cdot & & & \\ & & & \cdot & \cdot & \cdot & \cdot & & \\ & & & & \cdot & \cdot & \cdot & \cdot & \\ & & O & & & a_{-1} & a_0 & a_1 & a_2 \\ & & & & & & a_{-1} & a_0 & a_1 \\ & & & & & & & a_{-1} & a_0 \end{bmatrix} \tag{5.2}$$

where the matrix entries a_ℓ are given by (3.1b). This matrix is a banded Toeplitz matrix.

6. BANDED TOEPLITZ MATRICES

A Toeplitz matrix has the property that the entries are constant along diagonals parallel to the main diagonal. Our interest is in the eigenvalue spectrum for banded Toeplitz matrices of arbitrary order J. Since the eigenvalue analysis for triangular matrices is trivial, we restrict our attention to *non*-triangular matrices. The matrix bandwidth is $p + q + 1 (\leq J)$ where p and q are specified positive integers. Define the sequence

$$a_{-p}, a_{-p+1}, \cdots, a_0, \cdots, a_{q-1}, a_q; \quad \text{where} \quad a_{-p}, a_q \neq 0. \tag{6.1}$$

The elements of the banded Toeplitz matrix are given by

$$a_{ij} = a_{j-i} \tag{6.2}$$

if a_{j-i} is a member of the sequence (6.1) and zero otherwise.

As a particular example, if $p = 1$ and $q = 2$, then one obtains the banded Toeplitz matrix (5.2). In our applications the order J of the matrix is not fixed but is arbitrarily large. In particular for (5.2), we consider a sequence of quadridiagonal matrices of dimension J where J tends to infinity.

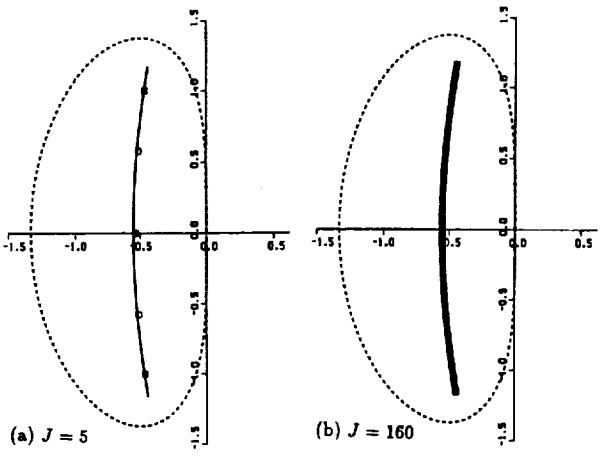

Fig. 6.1. Numerically computed eigenvalue spectra for the Toeplitz matrix (5.2).

If a Toeplitz matrix is tridiagonal, then the eigenvalues can be found analytically [8,1]. Also if a Toeplitz matrix is either upper or lower triangular (p or q =0), the eigenvalues are the diagonal elements. With these exceptions, the eigenvalues of banded Toeplitz matrices of arbitrary order J cannot, in general, be found analytically.

Eigenvalues of the Toeplitz matrix (5.2) were computed numerically (using an IMSL subroutine) and are plotted (open squares) in Fig. 6.1 for $J = 5$ and $J = 160$. The solid curve is the asymptotic spectrum for the same matrix. (The asymptotic spectra for the matrices (3.8b) and (5.2) are identical). For the matrix (5.2) there is no apparent numerical difficulty in computing the spectrum as J increases.

The transpose of the matrix (5.2) has the same eigenvalues as (5.2). However the numerical eigenvalue computations for the transposed matrix are adversely affected as demonstrated in Fig. 6.2. The eigenvalues should fall on the solid curve as shown for $J = 20$. But as J increases, the computed spectrum appears to approach the dashed oval curve which is the spectrum for the Cauchy problem (Section 7).

A non-normal Toeplitz matrix (e.g., (5.2)) can have the property that the eigenvalue spectrum is very sensitive to perturbations of the matrix elements. For such matrices, Trefethen [9] and Reichel and Trefethen [6] suggest that an eigenvalue analysis may lead to incorrect conclusions and it is more meaningful to analyze *pseudo*-eigenvalues. The *erroneous* eigenvalues plotted in Fig. 6.2 are a manifestation of the pseudo-spectra of the matrix $\mathbf{A}^T$ for increasing J.

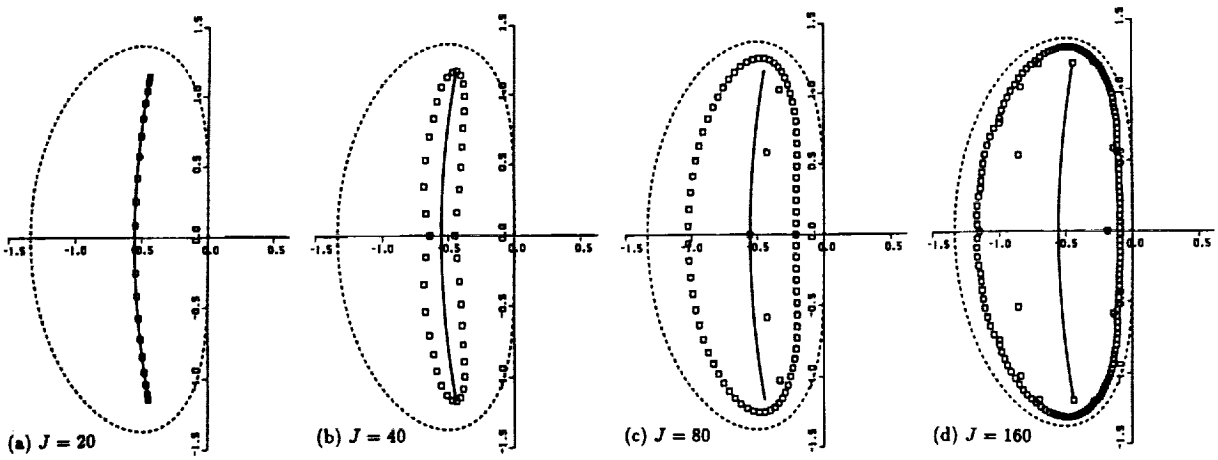

Fig. 6.2. Numerically computed eigenvalue spectra for the transpose of the Toeplitz matrix (5.2).

7. BANDED CIRCULANT (TOEPLITZ) MATRICES

A banded Toeplitz matrix is defined by the sequence (6.1) where $p + q + 1 \leq J$. Let the first row of a matrix of order J be

$$[a_0, a_1, \cdots, a_q, 0, \cdots, 0, a_{-p}, \cdots, a_{-2}, a_{-1}]. \tag{7.1}$$

Each row of a circulant matrix is constructed by cycling the previous row forward one element. This process defines the circulant *cousin* of a banded Toeplitz matrix. For example the circulant cousin of (5.2) is

$$\mathbf{C} = \begin{bmatrix} a_0 & a_1 & a_2 & & & & & a_{-1} \\ a_{-1} & a_0 & a_1 & a_2 & & & & \\ & a_{-1} & a_0 & a_1 & a_2 & & O & \\ & & \cdot & \cdot & \cdot & \cdot & & \\ & & & \cdot & \cdot & \cdot & \cdot & \\ & & & & \cdot & \cdot & \cdot & \cdot \\ & & O & & & a_{-1} & a_0 & a_1 & a_2 \\ a_2 & & & & & & a_{-1} & a_0 & a_1 \\ a_1 & a_2 & & & & & & a_{-1} & a_0 \end{bmatrix}. \tag{7.2}$$

A circulant matrix is also Toeplitz because the entries are constant along diagonals. The boundary conditions that lead to a circulant matrix are periodic.

In the context of discrete spatial approximations for the IBVP, the eigenvalue locus of a circulant Toeplitz matrix is coincident with the spectrum for the doubly infinite Toeplitz matrix [7] corresponding to a discrete pure initial-value or Cauchy problem.

The eigenvalues and eigenvectors of any circulant matrix can be found analytically. In particular, for the circulant matrix (7.2) with entries a_ℓ given by (3.1b), the eigenvalues are

$$\lambda_\ell = -\frac{4}{3}w_\ell^2 - i\left[1+\frac{2}{3}w_\ell\right]\sin\theta_\ell, \quad \text{where } w_\ell = \sin^2(\theta_\ell/2), \quad \theta_\ell = \frac{2\ell\pi}{J}, \quad \ell = 0, 1, \cdots, J-1. \tag{7.3}$$

The asymptotic eigenvalue spectrum is the *dashed* curve plotted in Fig. 3.1 and all subsequent figures.

It is a general result [7] that the eigenvalue spectrum of a banded Toeplitz matrix is *enclosed* by the spectrum of its circulant cousin (see e.g., Fig 3.1a).

8. BANDED QUASI-TOEPLITZ MATRICES

We start with a banded Toeplitz matrix defined by (6.2). A banded *quasi*-Toeplitz matrix is defined to be a Toeplitz matrix where there are a *few* row changes constrained as follows. There are at most p altered rows among the first p rows and at most q altered rows among the last q rows. Since p and q are fixed and J is assumed to be large, there are only a relatively few altered rows. Here we use *quasi* in the conventional sense meaning *almost* or *nearly*. For large J, the row alterations have only a *minimal* effect on the eigenvalue spectrum as one can see from the numerical examples of Section 13. The matrix (3.8b) is an example of a quasi-Toeplitz matrix with entry changes in the first and last rows.

9. EIGENVALUE PROBLEM FOR QUASI-TOEPLITZ MATRICES

A banded Toeplitz matrix with elements defined by (6.1) and (6.2) has lower bandwidth p and upper bandwidth q and the order of the matrix is J. The eigenvalue problem is defined by

$$\mathbf{A}\phi = \lambda\phi. \tag{9.1}$$

The eigenvalue problem (9.1) is equivalent to

$$\lambda\phi_j = \sum_{\ell=-p}^{q} a_\ell \phi_{j+\ell}, \quad j = 0, 1, \cdots, J-1 \tag{9.2}$$

with boundary conditions

$$\phi_{-\ell} = 0, \quad \ell = 1, 2, \cdots, p, \qquad \phi_{J+\ell} = 0, \quad \ell = 0, 1, \cdots, q-1. \tag{9.3a,b}$$

It is obvious that (9.2) is a generic row of (9.1).

Equation (9.2) is a $(p+q)$-th order difference equation for ϕ_j and we look for a solution of the form

$$\phi_j = \kappa^j \tag{9.4}$$

where κ is a complex constant. Insertion of (9.4) into (9.2) yields

$$\lambda = \sum_{\ell=-p}^{q} a_\ell \kappa^\ell. \tag{9.5}$$

This is an algebraic equation of degree $p+q$ in the unknown κ and in the following analysis we assume the roots are distinct. The general solution of (9.2) is

$$\phi_j = \sum_{\ell=1}^{p+q} \alpha_\ell \kappa_\ell^j \tag{9.6}$$

where the α_ℓ's are arbitrary constants. The constants α_ℓ are determined by inserting (9.6) into the boundary conditions (9.3). If the bandwidth is greater than three, the problem is analytically intractable.

For a quasi-Toeplitz matrix, the formulation of the eigenvalue problem is the same as above except that the boundary conditions are

$$q_\ell(E)\phi_{-\ell} = 0, \quad \ell = 1, 2, \cdots, p, \qquad w_\ell(E)\phi_{J+\ell} = 0, \quad \ell = 0, 1, \cdots, q-1. \quad (9.7a,b)$$

The subscripts on $q(E)$ and $w(E)$ indicate that the polynomial operators are, in general, different for each ℓ. In general, the eigenvalue problem for a quasi-Toeplitz matrix is analytically intractable.

10. PARTITION OF THE EIGENVALUE SPECTRUM

We assume that the order J of a quasi-Toeplitz matrix is large and we partition the eigenvalues into two groups. This partition is between (a) eigenvalues which are *independent* of the boundary conditions and (b) eigenvalues which are *dependent* on the boundary conditions. Group (b) may be empty.

We assume without loss of generality that the $p+q$ roots of the algebraic equation (9.5) are ordered as

$$|\kappa_1| \le |\kappa_2| \le \cdots \le |\kappa_p| \le |\kappa_{p+1}| \le \cdots \le |\kappa_{p+q}|. \quad (10.1)$$

The crucial inequality in (10.1) is the inequality between $|\kappa_p|$ and $|\kappa_{p+1}|$. As $J \to \infty$ there are only two choices: either

$$|\kappa_p| = |\kappa_{p+1}|, \qquad \text{or} \qquad |\kappa_p| < |\kappa_{p+1}|. \quad (10.2a,b)$$

This simple observation divides the asymptotic eigenvalue spectrum into two groups. In this section, we briefly describe the properties of the two groups. A more complete analysis is in [1].

We first consider the case of equality:

$$\text{group (a):} \qquad |\kappa_p| = |\kappa_{p+1}|. \quad (10.3)$$

For large J, the κ's of equal modulus (10.3) couple the left and right boundary conditions for the eigenfunction given by (9.6). On the other hand, the equality (10.3) allows one to find the eigenvalue spectrum which is *independent* of the boundary conditions. This may sound like a paradox, but the algorithmic details in the next section clarify how it is possible for the κ's and the spectrum to be independent of the boundary conditions.

Next we consider the inequality (10.2b):

$$\text{group (b):} \qquad |\kappa_p| < |\kappa_{p+1}|. \quad (10.4)$$

In this case, the left and right boundary conditions are uncoupled for large J. This fact is best clarified by an example. The algorithmic details are in the following section. Let $\bar{\kappa}$ denote the average modulus of the κ's of inequality (10.4), i.e.,

$$\bar{\kappa} = \frac{|\kappa_p| + |\kappa_{p+1}|}{2}. \quad (10.5)$$

Rescale the eigenvector (9.6) as

$$\tilde{\phi}_j = \frac{\phi_j}{\bar{\kappa}^j} = \sum_{\ell=1}^{p} \alpha_\ell \Big(\frac{\kappa_\ell}{\bar{\kappa}}\Big)^j + \sum_{\ell=p+1}^{p+q} \alpha_\ell \Big(\frac{\kappa_\ell}{\bar{\kappa}}\Big)^j. \tag{10.6}$$

For large j, say $j \approx J$, the first sum of the normalized eigenfunction (10.6) approaches zero near the right boundary since $|\kappa_\ell|/\bar{\kappa} < 1$ for $\ell \leq p$. Consequently, the second sum of the normalized eigenfunction (with q coefficients α_ℓ) must satisfy the right (q) boundary conditions independent of the first part of the eigenfunction. Conversely, the first part of the eigenfunction must satisfy the left (p) boundary conditions independent of the second part, i.e., the coefficients α_ℓ, $\ell = 1, 2, \cdots p$ are determined from the p boundary conditions given on the left boundary. In the limit $J \to \infty$, the independent sums with *nontrivial* coefficients correspond to boundary condition dependent eigenvalues and (in some cases) GKS quarter-plane eigenvalues.

Eigensolutions (modes) in group (b) depend intimately on the choice of boundary conditions and for certain choices there will be no eigensolutions in this group. One choice of boundary conditions which introduces no eigensolutions of group (b) is Dirichlet boundary conditions (9.3). Since Dirichlet boundary conditions lead to a pure Toeplitz eigenvalue problem, we conclude that *the spectrum for a pure Toeplitz matrix is composed only of the boundary condition independent eigenvalues.*

11. ALGORITHMS FOR THE EIGENVALUE SPECTRA OF QUASI-TOEPLITZ MATRICES

In this section we present algorithms for the asymptotic spectra of Toeplitz and quasi-Toeplitz matrices. We separate the algorithms according to the two groups of eigenvalues: (a) boundary condition independent (pure Toeplitz) and (b) boundary condition dependent. The application of each algorithm involves the solution of polynomials whose degree is proportional to the bandwidth $p+q+1$ of the matrix. A detailed description of the algorithms including numerical examples is in [1].

11.1 Boundary Condition Independent (Toeplitz) Spectrum

The algorithm for the pure Toeplitz spectrum is based on the observation that separated the spectrum into two groups, i.e., we seek those eigensolutions whose κ's satisfy (10.1) with the equality (10.3). We proceed as follows:
(i) Find all solutions of (9.5) with two distinct but equal modulus κ's. We denote these κ's by

$$\kappa_a = \hat{\kappa} e^{i\psi}, \quad \kappa_b = \hat{\kappa} e^{-i\psi}, \quad 0 < \psi < \pi \tag{11.1}$$

where $\hat{\kappa}$ is a complex variable. An equation for $\hat{\kappa}$ (independent of λ) is easily obtained. Since κ_a and κ_b each satisfy (9.5) we can eliminate λ and obtain a polynomial in $\hat{\kappa}$ with coefficients which are functions of the Toeplitz matrix coefficients and ψ.
(ii) For each ψ we must check that the κ's satisfy (10.1), i.e., that κ_a and κ_b are in fact κ_p and κ_{p+1}. For each $\hat{\kappa}$ we calculate κ_a and κ_b from (11.1), then calculate λ (and the remaining $p+q-2$ κ's) from (9.5). The λ is an eigenvalue in the Toeplitz spectrum if the $p+q$ κ's satisfy (10.1).

11.2 Boundary Condition Dependent Spectrum

The algorithm for the boundary condition dependent spectrum closely parallels the eigenvalue analysis of Kreiss [5] and Gustafsson, Kreiss, and Sundström [4]. There are however some differences since their analysis for hyperbolic initial-boundary-value problems makes two assumptions: (A) Cauchy stability (an assumption about the eigenvalues of the associated circulant Toeplitz matrix) and (B) the quarter-plane eigensolutions are *unstable* (i.e., the eigenvalues are in a particular portion of the complex plane). Since we are interested in the entire eigenvalue spectrum for any quasi-Toeplitz matrix, we do not impose conditions (A) and (B). The relaxation of these two conditions leads to a slightly more complicated algorithm.

The algorithm for the boundary condition dependent part of the spectrum is straightforward. We seek p (or q) values of κ which satisfy (9.5) and satisfy the left p (or right q) boundary conditions. The remaining q (or p) κ's must satisfy (10.1). The algorithm for the eigenvalues associated with the left boundary conditions is:
(i) Assume a solution of the form

$$\phi_j = \sum_{i=1}^{p} \alpha_\ell \kappa_\ell^j. \tag{11.2}$$

Substitute ϕ_j from (11.2) into the p left boundary conditions to obtain p equations for the κ_ℓ's and the α_ℓ's. The remaining equations are derived from the algebraic equation (9.5) since each of the p κ's must give the same value of λ.
(ii) After the p κ_ℓ's and corresponding λ are obtained, inequality (10.1) must be checked. This is accomplished by calculating the $p+q$ roots of (9.5) for the given λ and comparing those roots with the p κ_ℓ's. The λ is an eigenvalue in the boundary condition dependent part of the spectrum if (10.1) is satisfied.

The algorithm for the eigenvalues associated with the right boundary conditions is similar. Note that there may be no eigenvalues from the boundary condition dependent part of the spectrum even if non-Dirichlet boundary conditions are specified.

Although in principle the algorithms are straightforward, the algebra can become quite complicated if the bandwidth is even moderately large [1]. Kreiss [5] recognized that it is often very difficult to find GKS (i.e. unstable) eigenvalues by analytical methods. He proposed finding GKS eigenvalues (if they exist) by a numerical eigenvalue computation of the finite-domain problem where the boundary condition (or conditions) to be checked are on the left boundary and Dirichlet boundary conditions are imposed on the right boundary. Kreiss showed that GKS eigenvalues converge exponentially fast with increasing J. However, there may be difficulties in numerically delineating the GKS eigenvalues (or other boundary condition dependent eigenvalues) for *non-normal* matrices unless the matrix is rescaled as described in the following section.

12. EIGENVECTOR RESCALING

The difficulty in numerically computing the eigenvalues of a Toeplitz matrix (e.g., see Fig. 6.2) is due to exponentially growing eigenvectors. We illustrate this with an

example by considering the matrix (5.2). Since this is a Toeplitz matrix, the asymptotic spectrum is independent of the boundary conditions and the κ roots satisfy

$$|\kappa_1| = |\kappa_2| \leq |\kappa_3|. \tag{12.1}$$

For the roots of equal modulus one finds [1]

$$|\kappa_1| = |\kappa_2| = |\hat{\kappa}| \approx 1/\sqrt{3} \tag{12.2}$$

and consequently the moduli of the eigenvector elements behave as

$$|\phi_j| \approx (1/\sqrt{3})^j \tag{12.3}$$

i.e., they exponentially decrease with increasing j.

For the transpose $\mathbf{A}^T$ of (5.2) one has

$$|\check{\kappa}_1| \leq |\check{\kappa}_2| = |\check{\kappa}_3| \tag{12.4}$$

where the check symbol indicates that the κ's in (12.1) and (12.4) are not the same. In fact, the κ's of (12.1) and (12.4) are reciprocals. Consequently, for $\mathbf{A}^T$ one has

$$|\check{\kappa}_2| = |\check{\kappa}_3| = |\hat{\kappa}| \approx \sqrt{3} \tag{12.5}$$

and the moduli of the eigenvector elements

$$|\phi_j| \approx (\sqrt{3})^j \tag{12.6}$$

grow exponentially with increasing j.

A simple rescaling eliminates the exponentially growing eigenvectors. Let $\mathbf{A}$ denote an arbitrary banded Toeplitz matrix. If the κ's of equal modulus (10.3) are not on the unit circle, then either $\mathbf{A}$ or $\mathbf{A}^T$ will have exponentially growing eigenvectors. Assume that $\mathbf{A}$ has κ's of equal modulus (11.1) which are outside the unit circle. Define $\bar{\kappa}$ to be

$$\bar{\kappa} = \max_{0<\psi<\pi} (|\hat{\kappa}|). \tag{12.7}$$

For the matrix $\mathbf{A}$ we rescale the eigenvectors by

$$\tilde{\phi}_j = \frac{\phi_j}{\bar{\kappa}^j}. \tag{12.8}$$

The scaling is effectively a normalization of the $\hat{\kappa}$'s so their modului are approximately equal to unity. The *scaling* similarity matrix is diagonal (see [1] for details). If $a_{ij} = a_{j-i}$ are the nonzero elements of the Toeplitz matrix $\mathbf{A}$, the elements $\hat{a}_{ij}$ of the transformed matrix are

$$\hat{a}_{ij} = a_{j-i}\bar{\kappa}^{j-i}. \tag{12.9}$$

To numerically compute the eigenvalues of the rescaled eigenvalue problem, one simply replaces the matrix elements by (12.9).

In Fig. 12.1 we compare the computed eigenvalues of the unscaled and scaled Toeplitz matrix $\mathbf{A}^T$ where $\mathbf{A}$ is given by (5.2). This is the same example considered in Fig. 6.2d. If one starts with a quasi-Toeplitz matrix, then the appropriate scaling is the same as for the purely Toeplitz counterpart.

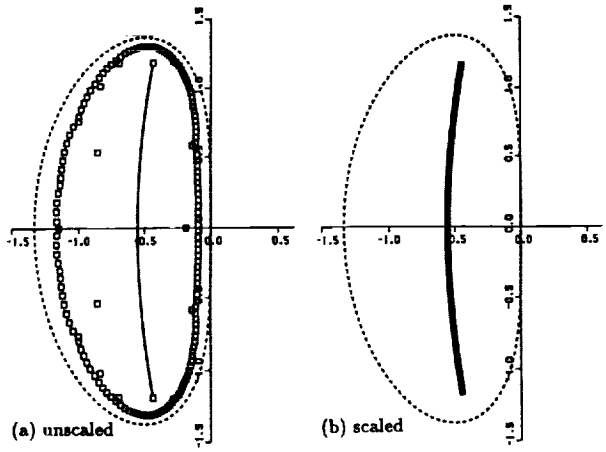

Fig. 12.1. Numerically computed eigenvalue spectra for the unscaled and scaled transpose of the Toeplitz matrix (5.2).

13. ADDITIONAL SPECTRAL PLOTS

The solid curve shown in all the previous plots, see e.g., Fig. 3.1, is the asymptotic spectrum for the Toeplitz matrix (5.2). The quasi-Toeplitz matrix (3.8b) has the same asymptotic spectrum since all the eigensolutions are in group (a) given by (10.3), i.e., there are no eigensolutions in group (b) given by (10.4). In practice we are interested in large finite values of J. In Fig. 13.1 we compare the asymptotic spectrum of the quasi-Toeplitz matrix (3.8b) with the discrete spectrum (open squares) for several values of J. For $J > 50$, the discrete spectrum falls on the asymptotic spectrum to within plotting accuracy.

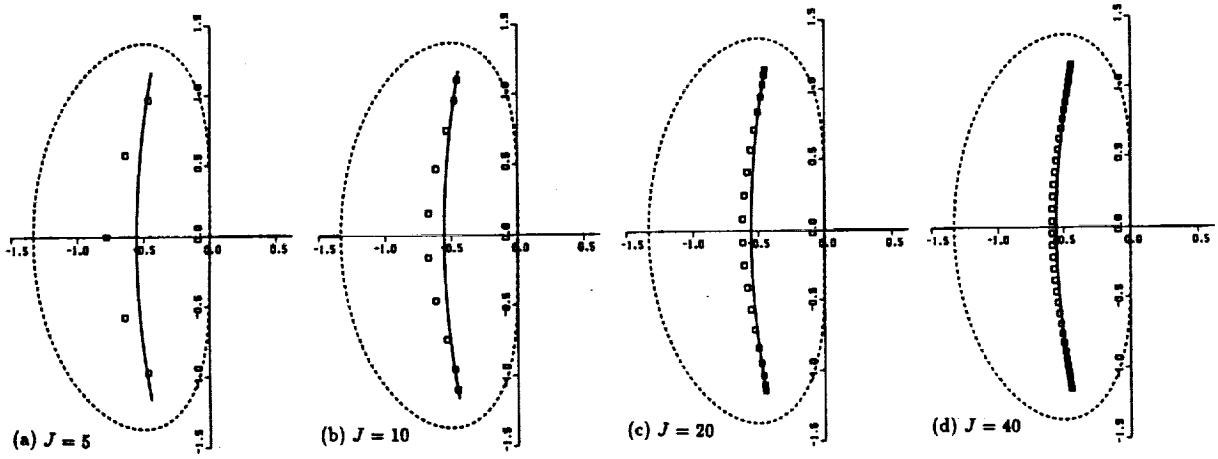

Fig. 13.1. Numerically computed eigenvalue spectra of the quasi-Toeplitz matrix (3.8b).

In order to illustrate eigenvalues which depend on the boundary conditions, we replace the NBS (3.5) by (3.9). In the remainder of this section, the quasi-Toeplitz matrix is (3.8b) with the last row replaced by $[0, 0, \cdots, c_{-2}, c_{-1}, c_0]$ where the c_ℓ's are given as a function of the parameter β by (3.9b). By applying the eigenvalue analysis to the semi-discrete approximation with the NBS (3.9), one finds that there are no boundary

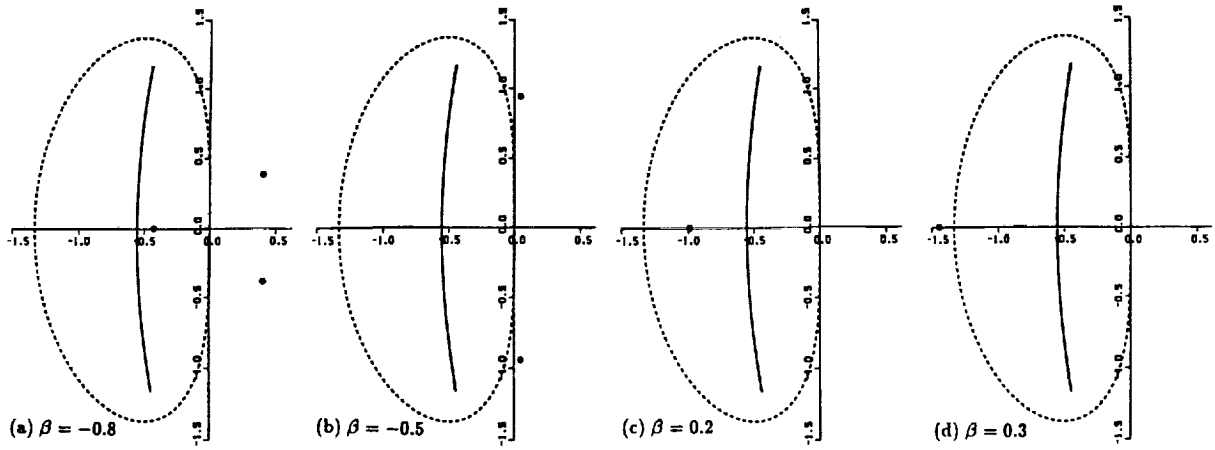

Fig. 13.2. Asymptotic eigenvalue spectra for a quasi-Toeplitz matrix.

condition dependent eigenvalues for $-0.84 \leq \beta \leq 0.167$ and the approximation is GKS unstable for $\beta \leq -0.48$ [1].

In Fig. 13.2 we show the asymptotic spectra computed for several values of β using the algorithms of Section 11. The filled circles depict boundary condition dependent eigenvalues. The filled circles to the right of the imaginary axis (Figs 13.2a,b) correspond to GKS eigenvalues. For $\beta = -0.8$ or -0.5, the discrete IBVP is GKS unstable. One can have boundary condition dependent eigenvalues which do not lead to instability. These eigenvalues are not considered in the GKS theory. The filled circles to the left of the imaginary axis in Figs. 13.2a,c,d correspond to non-GKS eigenvalues. For $\beta = 0.2$ or $\beta = 0.3$, the discrete IBVP is GKS stable. In Fig. 13.2a,b,d we show boundary condition dependent eigenvalues which are outside the Cauchy spectrum. Thus although the Toeplitz part of the spectrum is contained inside the Cauchy spectrum, there are boundary condition dependent eigenvalues outside the Cauchy spectrum.

It is worth noting that if one were to compute the eigenvalues numerically for increasing J (using the *rescaled* matrix), the GKS and non-GKS numerical eigenvalues would fall to plotting accuracy on the filled circles in Fig. 13.2. Therefore (with the possible exception of GKS generalized eigenvalues) the stability of discrete approximations to IBVP's can be inferred from a numerical computation of the finite-domain eigenvalues provided the matrix is rescaled as described in Section 12.

14. CONCLUSIONS

The eigenvalue analysis for a discrete hyperbolic IBVP reduces to the eigenvalue analysis of a quasi-Toeplitz matrix. We have devised an algorithm to determine the asymptotic spectrum of any banded quasi-Toeplitz matrix. The method used in the analysis partitions the eigenvalues into two groups. The partition is between eigenvalues independent of the boundary conditions and eigenvalues dependent on the boundary conditions. For each group of eigenvalues a computational algorithm is given. The spectrum independent of the boundary conditions is associated with an auxiliary Dirichlet problem (banded Toeplitz matrix). The method used to find the asymptotic spectrum also leads to a simple similarity transformation so that reliable numerical eigenvalue computations can be made for banded Toeplitz and quasi-Toeplitz matrices of any order.

Our original interest was in the eigenvalue spectrum of quasi-Toeplitz matrices arising from discrete approximations of hyperbolic IBVPs. However, the algorithm developed in this paper is independent of the origin of the quasi-Toeplitz matrix. Consequently, the computational algorithm of Section 11 is also valid for convection-diffusion IBVPs or for banded Toeplitz or quasi-Toeplitz matrices which do not arise from discrete approximations to partial differential equations.

REFERENCES

[1] R. M. Beam, R. F. Warming, "The eigenvalue spectra of banded Toeplitz and quasi-Toeplitz matrices," to appear.

[2] S. K. Godunov, V. S. Ryabenkii, "Special stability criteria of boundary value problems for non-selfadjoint difference equations," Russ. Math. Surv., 18, [1963], pp. 1-12.

[3] B. Gustafsson, "The convergence rate for approximations to mixed initial boundary value problems," Math. Comp., 29, [1975], pp. 396-406.

[4] B. Gustafsson, H.-O. Kreiss, A. Sundström, "Stability theory of difference approximations for mixed initial boundary value problems. II," Math. Comp., 26, [1972], pp. 649-686.

[5] H.-O. Kreiss, "Stability theory for difference approximations of mixed initial boundary value problems. I," Math. Comp., 22, [1968], pp. 703-714.

[6] L. Reichel, L. N. Trefethen, "Eigenvalues and pseudo-eigenvalues of Toeplitz Matrices", Numer. Math., to appear.

[7] P. Schmidt and F. Spitzer, "The Toeplitz matrices of an arbitrary Laurent Polynomial," Math. Scand., 8, [1960], pp. 15-38.

[8] G. D. Smith, "Numerical Solution of Partial Differential Equations: Finite Difference Methods," Oxford University Press, Oxford, [1978], pp. 113-115.

[9] L. N. Trefethen, "Non-normal matrices and pseudo-eigenvalues in numerical analysis," to appear.

[10] R. F. Warming, R. M. Beam: "An eigenvalue analysis of finite-difference approximations for hyperbolic IBVPs," Notes on Numerical Fluid Mechanics, 29, edited by P. Wesseling, Vieweg, Braunschweig, [1990], pp. 564-573.

NASA
National Aeronautics and Space Administration

Report Documentation Page

1. Report No.	2. Government Accession No.	3. Recipient's Catalog No.
NASA TM-102874		

4. Title and Subtitle
An Eigenvalue Analysis of Finite-Difference Approximations for Hyperbolic IBVPs II: The Auxillary Dirichlet Problem

5. Report Date
November 1990

6. Performing Organization Code

7. Author(s)
Robert F. Warming and Richard M. Beam

8. Performing Organization Report No.
A-90311

10. Work Unit No.
505-60

9. Performing Organization Name and Address
Ames Research Center
Moffett Field, CA 94035-1000

11. Contract or Grant No.

13. Type of Report and Period Covered
Technical Memorandum

12. Sponsoring Agency Name and Address
National Aeronautics and Space Administration
Washington, DC 20546-0001

14. Sponsoring Agency Code

15. Supplementary Notes
Point of Contact: Robert F. Warming, Ames Research Center, MS 202A-1, Moffett Field, CA 94035-1000; (415) 604-5215 or FTS 464-5215
Presented at the Third International Conference on Hyperbolic Problems, June 11-15, 1990, Uppsala, Sweden.

16. Abstract

The matrix eigenvalue problem for a discrete hyperbolic initial-boundary-value problem reduces to the eigenvalue analysis of a banded quasi-Toeplitz matrix. A direct analysis is, in general, analytically intractable and numerically unreliable. An asymptotic (large matrix order) approach partitions the eigenvalue analysis into two parts, namely the analysis for the boundary condition *independent* eigenvalues and the analysis for the boundary condition *dependent* eigenvalues. The boundary condition independent spectrum is associated with an auxiliary Dirichlet problem, i.e., the spectrum of a banded Toeplitz matrix. The boundary condition dependent spectrum is associated with the normal modes of the Godunov-Ryabenkii and the Gustafsson-Kreiss-Sundström stability theory; however, eigenvalues not considered in the stability theory (i.e., *stable* eigenvalues) may be part of the boundary condition dependent spectrum. In this paper we describe a method for determining the eigenvalue spectra for banded Toeplitz and quasi-Toeplitz matrices of large order. The algorithm for the asymptotic spectrum also leads to a simple similarity transformation that allows reliable numerical eigenvalue computations for banded Toeplitz and quasi-Toeplitz matrices of any order.

17. Key Words (Suggested by Author(s))	18. Distribution Statement
Stability, Hyperbolic, Finite-difference approximations, Eigenvalues, Toplitz matrices	Unclassified-Unlimited Subject Category - 64

19. Security Classif. (of this report)	20. Security Classif. (of this page)	21. No. of Pages	22. Price
Unclassified	Unclassified	19	A02